Journal of Orthopaedic Translation 47 (2024) 74–86

Contents lists available at ScienceDirect

Journal of Orthopaedic Translation

journal homepage: www.journals.elsevier.com/journal-of-orthopaedic-translation

Original Article

Augmentation of functional recovery via *ROCK/PI3K/AKT* pathway by Fasudil Hydrochloride in a rat sciatic nerve transection model

Hai Wang [a,b,1], Fang Fang [d,1], Xing jing [c], Dan Xu [c], Zhenyu Ren [a,b], Shuang Dou [c], Yun Xie [a,b,*], Yuehong Zhuang [c,**]

[a] *Department of Orthopedics, First Affiliated Hospital, Fujian Medical University, Fuzhou, 350004, Fujian, China*
[b] *Department of Orthopedics, National Regional Medical Center, Binhai Campus of the First Affiliated Hospital, Fujian Medical University, Fuzhou, 350212, China*
[c] *Fujian Key Laboratory of brain aging and neurodegenerative diseases, institute of clinical applied anatomy, the school of basic medical sciences, Fujian medical university, Fuzhou, 350108, Fujian, China*
[d] *Department of pharmacology, Fujian medical university, Fuzhou, 350108, China*

ARTICLE INFO

Keywords:
Fasudil
PI3K/AKT
Rho kinase
Sciatic nerve transection injury

ABSTRACT

Backgrounds: The functional recovery after peripheral nerve injury remains unsatisfactory. This study aims to perform a comprehensive evaluation of the efficacy of Fasudil Hydrochloride at treating the sciatic nerve transection injury in rats and the mechanism involved.

Materials and methods: In animal experiments, 75 Sprague Dawley rats that underwent transection and repair of the right sciatic nerve were divided into a control, Fasudil, and Fas + LY group, receiving daily intraperitoneal injection of saline, Fasudil Hydrochloride (10 mg/kg), and Fasudil Hydrochloride plus LY294002 (5 mg/kg), respectively. At day 3 after surgery, the expression of ROCK2, p-PI3K, and p-AKT in $L_{4\text{-}5}$ DRG and the lumbosacral enlargement was determined using Western blotting. At day 7 and 14, axon density in the distal stump was evaluated with immunostaining using the anti-Neurofilament-200 antibody. At day 30, retrograde tracing by injecting Fluoro-gold in the distal stump was performed. Three months after surgery, remyelination was analyzed with immostaining using the anti-MPZ antibody and the transmission electron microscope; Moreover, Motion-Evoked Potential, and recovery of sensorimotor functions was evaluated with a neuromonitor, Footprint, Hot Plate and Von Frey Filaments, respectively. Moveover, the Gastrocnemius muscles were weighed, and then underwent H&E staining, and staining of the neuromuscular junction using α-Bungarotoxin to evaluate the extent of atrophy and degeneration of the endplates in the Gastrocnemius. In vitro, spinal motor neurons (SMNs) and dorsal root ganglia (DRG) were cultured to examine the impact of Fasudil Hydrochloride and LY294002 on the axon outgrowth.

Results: Three days after injury, the expression of ROCK2 increased significantly ($P < 0.01$), and Fasudil application significantly increased the expression of p-PI3K and p-AKT in $L_{4\text{-}6}$ DRG and the lumbosacral enlargement ($P < 0.05$). At day 7 and 14 after surgery, a higher axon density could be observed in the Fasudil group($P < 0.05$). At day 30 after surgery, a larger number of motor and sensory neurons absorbing Fluoro-gold could be observed in the Fasudil group ($P < 0.01$) Three months after surgery, a greater thickness of myelin sheath could be observed in the Fasudil group ($P < 0.05$). The electrophysiological test showed that a larger amplitude of motion-evoked potential could be triggered in the Fasudil group ($P < 0.01$). Behavioral tests showed that a higher sciatic function index and a lower threshold for reacting to heat and mechanical stimuli could be measured in the Fasudil group. ($P < 0.01$). The wet weight ratio of the Gastrocnemius muscles and the area of the cross section of its myofibrils were greater in the Fasudil group ($P < 0.01$), which also demonstrated a higer ratio of axon-endplate connection and a larger size of endplates ($P < 0.05$). And there were no significant differences for the abovementioned parameters between the control and Fas + LY groups ($P > 0.05$). In vitro studies showed

* Corresponding author. Department of Orthopedics, First Affiliated Hospital, Fujian Medical University, Fuzhou, 350004, Fujian, China.
** Corresponding author. Fujian Key Laboratory of Brain Aging and Neurodegenerative Diseases, Institute of Clinical Applied Anatomy, The School of Basic Medical Sciences, Fujian Medical University, Fuzhou, 350108, Fujian, China.
E-mail addresses: xieyun@fjmu.edu.cn (Y. Xie), Zhuangyuehong@163.com (Y. Zhuang).
[1] **Hai Wang and Fang Fang** made equal contributions to this study and should serve as the co-first authors

https://doi.org/10.1016/j.jot.2024.06.006
Received 8 April 2024; Received in revised form 18 May 2024; Accepted 3 June 2024

that Fasudil could significantly promote axon growth in DRG and SMNs, and increase the expression of p-PI3K and p-AKT, which could be abolished by LY294002 ($P < 0.05$).
Conclusions: Fasudil can augment axon regeneration and remyelination, and functional recovery after sciatic nerve injury by activating the PI3K/AKT pathway.
The translational potential of this article: The translation potential of this article is that we report for the first time that Fasudil Hydrochloride has a remarkable efficacy at improving axon regeneration and remyelination following a transection injury of the right sciatic nerve in rats through the ROCK/PI3K/AKT pathway, which has a translational potential to be used clinically to treat peripheral nerve injury.

Peripheral nerve injuries (PNI) are estimated to occur between 1.46 % and 2.8 % of multiple trauma patients, or 5 % if root and plexus injuries are included [1,2]. Among the various forms of injury, peripheral nerve transection is one of the most common manifestations that can be caused by a cutting object [3]. Significant advancements have been made in the technique of microsurgery for injured nerves that sometimes result in improved outcome for patients [4]. Unfortunately, functional recovery is often still poor, especially when nerve trunks close to the spinal cord and far from the target organs are injured [5]. After these types of nerve injuries, injured neurons are required to regenerate their axons over long distances at a very slow rate of 1 mm/d [6]. At this sluggish rate of regeneration, reestablishment of a functional motor unit or sense organ reinnervation may take months or even years, a condition referred to as chronic axotomy [7]. Likewise, if Schwann cells in the distal nerve stumps and the target organs remain denervated for long periods, the conditions are known as chronic denervation of Schwann cells [8,9] and chronic muscle denervation [4,10], respectively, which will undergo irreversible fibrosis that will prevent subsequent reinnervation and regain of function. Therefore, augmenting axon regeneration to reduce the risk of chronic axotomy and improve functional recovery after PNI is of great clinical importance.

RhoA is a small GTPase protein and belongs to Rho GTPase family. RhoA mediates the formation of focal adhesion and stress fibers, which are contractile acting bundles in non-muscle cells that regulate cell contractility, providing force for cell adhesion, migration, and morphogenesis [11,12]. Therefore, inhibiting RhoA or ROCK has been reported to be able to augment axon growth [13]. Meanwhile, the PI3K/AKT pathway has been showed to be activated by inhibition of RhoA/ROCK with miRNAs: Xiao reported that MiR-133b can promote neurite outgrowth in vitro by inhibiting Rho A and activating the PI3K/AKT pathway [14]. Gu reported that miR-124 can repress ROCK1 expression to promote neurite elongation through activation of the PI3K/Akt signal pathway [15].

Fasudil, a specific ROCK inhibitor, has been successfully used in clinical practice for the treatment of subarachnoid hemorrhage in Japan [16]. Increasing bodies of evidence suggested that Fasudil could exhibit remarkable therapeutic effect on the disorders of the central nervous system [17–21]. However, there are few investigations dedicated to a comprehensible evaluation of the efficacy of Fasudil at improving functional recovery after severe PNI. In this study, we set out to examine the impact of Fasudil on axonal regeneration, remyelination, functional recovery, and whether PI3K/AKT serves as a downstream mediator in a rat sciatic nerve transection model.

1. Materials and methods

75 male Sprague–Dawley rats, weighing 201 ± 30g, were used in this study. The study was carried out in accordance with the ARRIVE guidelines, and following the National Research Council's Guide for the Care and Use of Laboratory Animals. After anaesthesia, the hair of the right lower limb was shaved and disinfected, and incisions were made through the skin and the right gluteus maximus to expose the right sciatic nerve. Then, iris scissors were used to transect the sciatic nerve just distal to the inferior margin of the biceps femoris (Figs. 1 and 2). Afterwards, a 10-0 nylon suture was used to stitch together the epineurium of the proximal and distal stumps at four points (0°, 90°, 180°, and 270°). Finally, the muscles and skin were sutured sequentially to close the wound.

The 75 rats were then randomly and evenly divided into a control group, a Fasudil group, and a Fas + LY group. Each group underwent daily intraperitoneal injection with normal saline, Fasudil Hydrochloride (ROCK inhibitor,10 mg/kg, F912038, Macklin), or Fasudil Hydrochloride (10 mg/kg) plus LY294002 (PI3K inhibitor, 5 mg/kg, L832989, Macklin), respectively. At day 3, 1, 2, 4, and 12 weeks after treatment, five rats from each group were sacrificed for assays of various purposes.

2. Immunofluorescent and histological staining

At the 1, 2, 4 and 12 weeks after surgery, five rats in each time point of the three groups were subjected to transcardial perfusion, and the sciatic nerves were harvested and immersed in 4 % paraformaldehyde for 24h before being moved to 30 % glucose for dehydration. Afterwards, routine cryosection with a thickness of 15um was performed, and immunofluorescent staining was carried out with the following protocol: the frozen sections were rinsed 2 times with PBS for 10 min each, and permeated with 0.1 % triton x-100 in PBS for 10 min, and then blocked in 5 % normal goat serum in PBS (pH 7.4) for 1h. Afterwards, sections were incubated with primary antibodies at 4 °C overnight, and then with

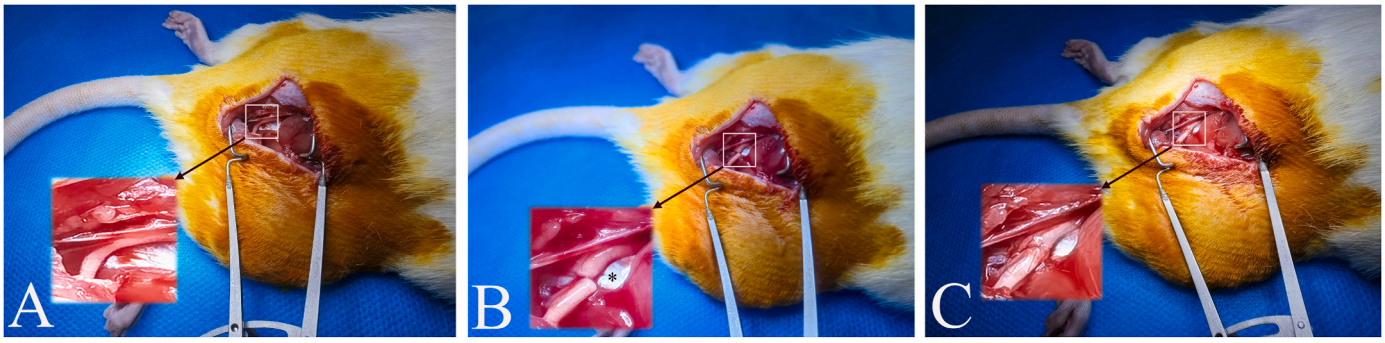

Fig. 1. Establishment of the sciatic nerve transection model. A, split of the gluteus maximus to expose the right sciatic nerve; B, transect the sciatic nerve at the inferior margin of the biceps femoris; C, stitch together the proximal and distal stumps of the nerve using a 10-0 nylon suture at four points.

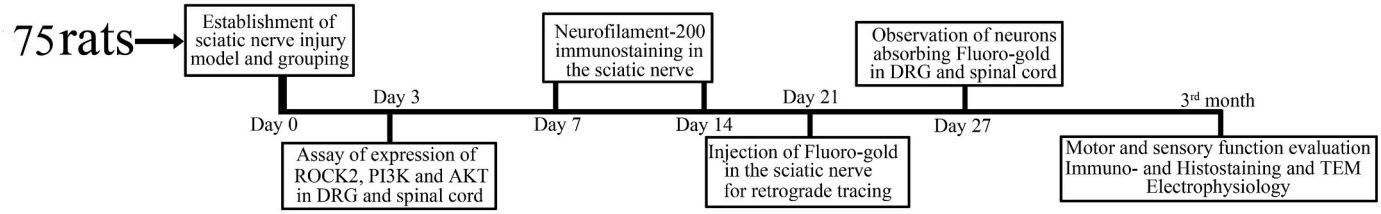

Fig. 2. Flow chart of the animal experiment. 75 rats were used in this study, and divided to the control, Fasudil and Fasudil + LY294002 groups after model establishment. 15 rats with five from each group were then sacrificed at each of the five time points, and tissues harvested for different assays.

secondary antibodies for 1h at room temperature. Rinsing was performed in PBS (pH 7.4) between all steps. The same protocol was adopted for immunostaining of neurons after fixation with 4 % paraformaldehyde for 10min. Primary antibodies used included antibodies against Neurofilament-200-FITC (NF-200, Sigma, SAB4200811, 1:200), myelin protein zero (MPZ, Beyotime, AF7497, 1:1000), NeuN (Proteintech, 26975-1-AP, 1:500), neuron-specific Class III β-tubulin (Tuj 1, Covance, MMS-435P, 1:500), ChaT (Beyotime, AF6497,1:500). The secondary antibodies used included the goat anti-rabbit IgG H&L488 (abcam, ab96883, 1:1000), goat anti-mouse IgG H&L cy3 (Beyotime, A0521, 1:500) antibodies. Histochemical staining for observation of the neuromuscular junction using α-Bungarotoxin (Invitrogen, B35450) was also performed.

2.1. Western blotting

At day 3 after model establishment, the $L_{4\text{-}6}$ DRG and the lumbosacral enlargement from the rats were harvested. And three days after culture, 20 plus DRG explants and 1×10^6 SMNAs from each groups were collected. 300ul NP-40 containing 1ul phenylmethylsulfonyl fluoride (100umol) and 0.1ul protease and phosphatase inhibitors were added to the tissues or cells, respectively. The homogenate was centrifuged at 14,000×*g* for 15 min. The supernatant was aspirated. Protein concentration was determined using a bicinchoninic acid (BCA) kit. Equal amounts of protein (20ug) was separated by 10 % sodium dodecyl sulfate-polyacrylamide gel and transferred onto a polyvinylidene difluoride membrane (Millipore, Massachusetts, USA). After incubation with blocking buffer for 2 h at room temperature, the membrane was incubated with primary antibodies against PI3K (1:1,000, CST, 4257), P-PI3K (1:1,000, CST, 4228), AKT(1:1,000, Abcam, ab179463), P-AKT (1:1,000, CST, 9271) and ROCK2(1:1,000, Proteintech, 20248-1-AP), and beta-Actin (1:1,000, Beyotime, AF5006) overnight at 4 °C. After washing off the unattached primary antibodies with Tris Buffered Saline with Tween 20 (TBST), the membrane was incubated in the presence of secondary HRP-conjugated Affinipure Goat Anti-Rabbit IgG(H + L) (1:1000, proteintech, SA00001-2) for 2 h at room temperature. then, the membrane was washed with TBST. The membrane was developed by enhanced chemiluminescence (Beyotime). Band intensities were quantified by Image J and normalized against the loading control. Each assay was repeated three times.

3. Retrograde tracing with Fluoro-gold

At three weeks after surgery, the right sciatic nerves of five rats in each group were exposed after anesthesia, and 5ul of Fluoro-gold (sc-358883, Santa Cruz) was injected into each sciatic nerve at 1 cm distal to the transection site with a 10ul HAMlLTON syringe. Then, the incisions were sutured and the rats were kept alive for one week. Afterwards, the rats were sacrificed, and the lumbosacral enlargement and $L_{4\text{-}6}$ dorsal root ganglia were harvested for cryosection with a thickness of 50um. The tissues sections were placed on slides and washed with PBST twice for 10min each, and then with PBS once for 10min. Then the slides were placed under a fluorescent microscope, and observed and photographed using the ultraviolet excitation light. The neurons absorbing Fluoro-gold in one of every four continuous sections were counted, and added up as the total number of neurons absorbing Fluoro-gold in a rat.

4. Evaluation of functional recovery

At 12 weeks after model establishment, the motor and sensory recovery of the injured hind limbs were evaluated. The motor function was evaluated with the Sciatic Function Index (SFI). In brief, a self-made walking track underlined with pieces of white paper was set up for the rats to pass, leaving footprints. Several measurements were taken: the distance from the heel to toe, the print length (PL); the distance from the first to fifth toes, the toe spread (TS); and the distance between the second and fourth toes, the intermediary toe spread (IT). These data were collected for both the normal (N) and experimental (E) feet.The SFI was calculated using the formula: $SFI = -38.3 \times (EPL\text{-}NPL)/NPL + 109.5 \times (ETS\text{-}NTS)/NTS + 13.3 \times (EIT\text{-}NIT)/NIT\text{-}8.8$.

The recovery of mechanical and thermal sensation was evaluated using Von Frey filaments and Hot Plate, respectively. To test using Von Frey filaments, the rats were placed in a wire mesh cage and allowed to acclimate to the environment for 10 min. After settling down of the rats, a series of standardized Von Frey filaments were applied perpendicularly to the plantar area of the injured hind paw for 5 s. If a quick withdrawal response was evoked during or immediately after removing the fiber, it was recorded as a positive response; Otherwise, it was recorded as a negative response.

The temperature of the hot plate was set at 55 ± 5 °C. Each rat was placed on the hot plate and the average time for the rat to lick the affected hind paw was recorded, which indicated the response time of the rat to hot stimulation. Three measurements were taken and averaged to represent the response time of the rat. Each measurement was separated by 5 min and the test duration was not allowed to exceed 60 s to prevent the rat from being burned. If there was no response after 60 s, it was recorded as 60 s.

4.1. Motion-Evoked Potential

Under aseptic conditions, transcranial motor-evoked potential stimuli were applied with a transcranial electrical stimulator through two needle electrodes attached to the scalp at the intensity of 50V and 100 mA. At the same time, two recording needle electrodes were inserted into the Gastrocnemius on the right, and two reference needle electrodes were inserted into the healthy Gastrocnemius. A grounding electrode was placed over the tail. An intraoperative neuromonitor (NIM-Eclipse) was used to record the evoked potential.

5. Evaluation of muscle atrophy

At 12 weeks, the rats were sacrificed, and the bilateral Gastrocnemius muscles were exposed, resected and weighed. The wet weight ratio of the right Gastrocnemius was calculated by dividing the weight of the Gastrocnemius from the right side to that of the left side. After weighing, the Gastrocnemius muscles was frozen immediately in a mixture of acetone and dry ice, and then transferred a −80 °C refrigerator for long-term store. The frozen muscles were subjected to cryosection with a

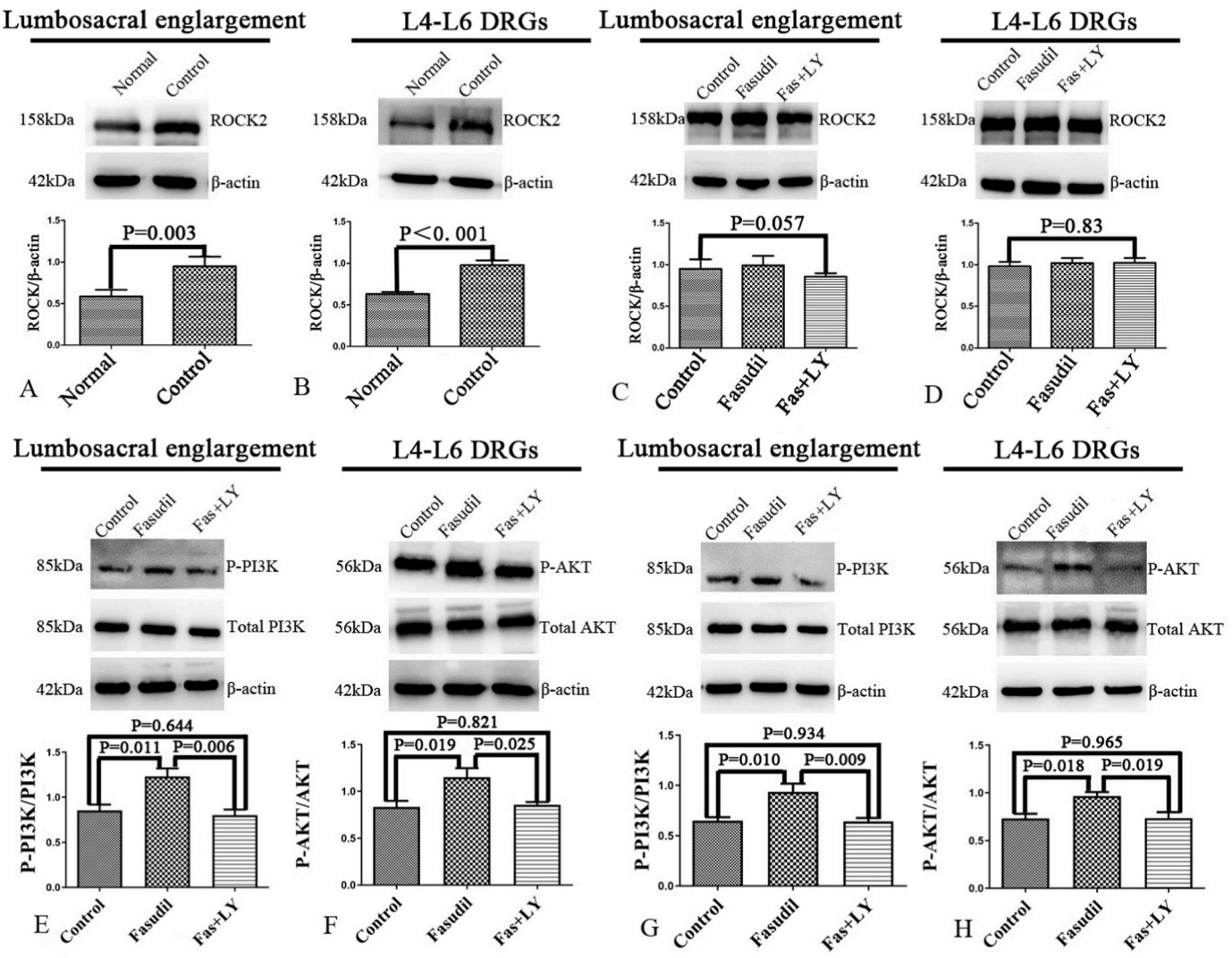

Fig. 3. Assay of expression of ROCK2, PI3K, and AKT at day 3 after establishment of the transection model. A and B showed that the expression of ROCK2 was significantly up-regulated in both the lumbosacral enlargement and DRG compared to that in rats with sham surgery; C and D showed that application of Fasudil did not directly inhibit the expression ROCK2; E, F, G and H showed that application of Fasudil could significantly increase the phosphorylation of PI3K and AKT in the lumbosacral enlargement and DRG.

thickness of 30 μm sections, and underwent hematoxylin and eosin (H&E) staining of muscles using a test kit (Solarbio, G1120). The cross area of myofibrils in three fields of each section captured with a light microscope under 20× magnification was measured using Image J (National Institutes of Health) and averaged to represent the cross area of the individual myofibril of each rat.

6. Transmission electronic microscopy (TEM)

At 12 weeks after surgery, 2-mm long segments from an area 5 mm distal to the injury site were post-fixed with 2.5 % glutaraldehyde plus 2 % paraformaldehyde for 24 h followed by 1 % OsO^4 for 2 h at 4 °C, dehydrated stepwise in increasing concentrations of acetone and embedded in resin for ultrathin transverse sectioning. After staining with 2 % uranyl acetate and lead citrate, ultrathin sections were observed under a transmission electron microscope (H-7500, Hitachi). Three images of each sample were randomly captured at a magnification of 6000. Then, the thickness of the myelin in each image was measured with Image J and averaged to represent the thickness of myelin in a rat.

7. Harvest of dorsal root ganglia(DRG)

DRG explants from the spinal cords of day-15 rat embryos were isolated and cultured as described by Xu [22].The DRG explants were divided into six groups: a control group, a Fasudil group, a Fas + LYgroup, a CSPG group, a CSPG + F group, and a CSPG + F + LYgroup, with five DRG explants in each group. In the former three groups, the DRG explants were seeded to a 24-well plate coated with poly-ᴅ-lysine (PDL, 20ug/mL, Sigma–Aldrich, P6407) mimicking a permissive environment, whereas in the latter three groups the DRG explants were seeded to the plate coated with PDL and CSPG (Chondroitin sulfate proteoglycan , 2.5ug/mL, CC117, Sigma Aldrich) mimicking a non-permissive environment. In the Fasudil group and the CSPG + F group, 10umol/L of Fasudil Hydrochloride was added to the culture medium. In the Fas + LY group and the CSPG + F + LY group, 10 umol/L Fasudil plus 10 umol/L LY294002 were added to the culture medium. At day 3, the proteins were extracted for determining the phosphorylation level of PI3K and AKT. At day 5, immunofluorescent staining using the anti-β-tubulin antibody (1:500, Beyotime, AT809) was used to better display the axons. In each DRG explant, the length of axon at four angles (0°, 90°, 180°, and 270°) were measured and averaged to represent the axon length of the DRG.

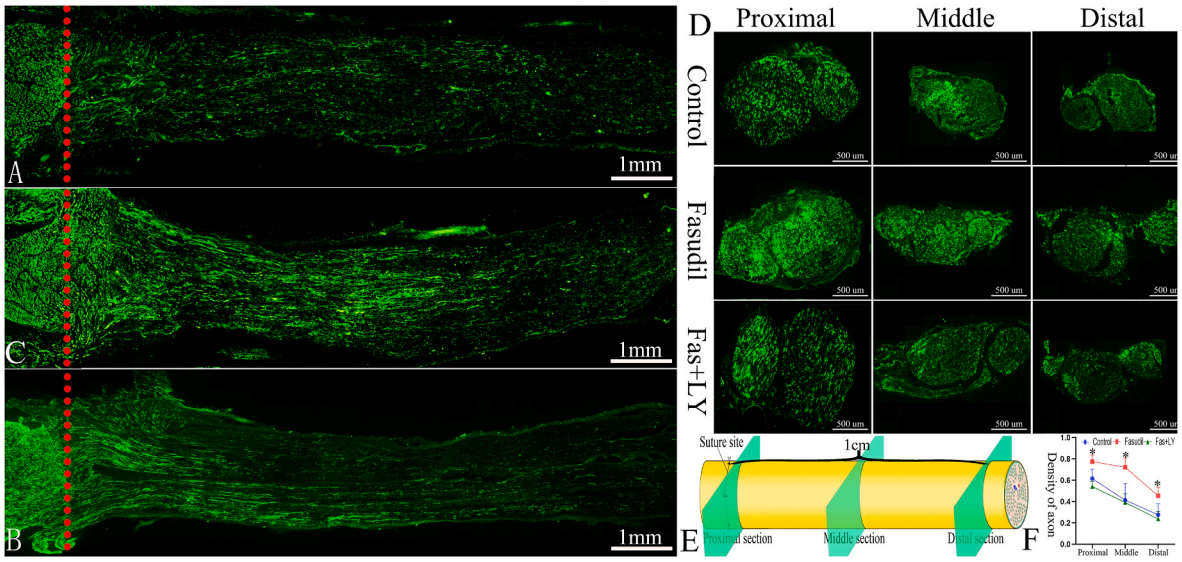

Fig. 4. Immunofluorescent staining of NF-200 in longitudinal and cross sections of the sciatic nerve 1 and 2 weeks after surgery. A, B and C were the longitudinal sections of the sciatic nerves 1 week after surgery in the control, Fasudil and Fas + LY, respectively. The red dotted lines represented the sites of transection. D was the proximal, middle, and distal cross sections of the sciatic nerves 1 cm distal to the suture site 2 weeks after surgery as indicated in E. As indicated in F, the axonal density was significantly higher in the Fasudil group than that in the other two groups(*denotes P < 0.05). (For interpretation of the references to colour in this figure legend, the reader is referred to the Web version of this article.)

8. Extraction and culture of spinal motor neurons (SMNs)

SMNs were prepared from day-15 embryonic rats with an immunopanning protocol from Graber and Harris [23]. The cells were divided into six groups as described above. The "permissive" coating included 20ug/mL of PDL for 30min, followed by the addition of 0.3 mL of human placental laminin (Sigma–Aldrich, L6274), mimicking a permissive environment, and the "non-permissive" coating included PDL(20ug/mL) and CSPG (2.5ug/mL) for 30min, followed by the addition of 0.3 mL of laminin. The extracted motor neurons were cultured at a density of 5000 cells per well, and Fasudil Hydrochloride and LY294002 were added to the culture medium in the same way as described above. Each group had five wells of neurons. At day 3, the proteins were extracted for determining the phosphorylation level of PI3K and AKT. At day 5, immunofluorescent staining using the anti-β-tubulin antibody (1:500, Beyotime, AT809) was used to better display the axons. Eight fields were photographed for each well. The axon length of the neurons in each field was measured, and averaged to represent the axon length of the neurons in the well.

8.1. Statistical analysis

All data in this study were expressed in the form of Mean ± Std. One-way ANOVA was adopted for detection of statistical differences among the groups with LSD or Dunnett's T3 adopted for post-hoc comparisons depending on the homogeneity of variance. A P value lesser than 0.05

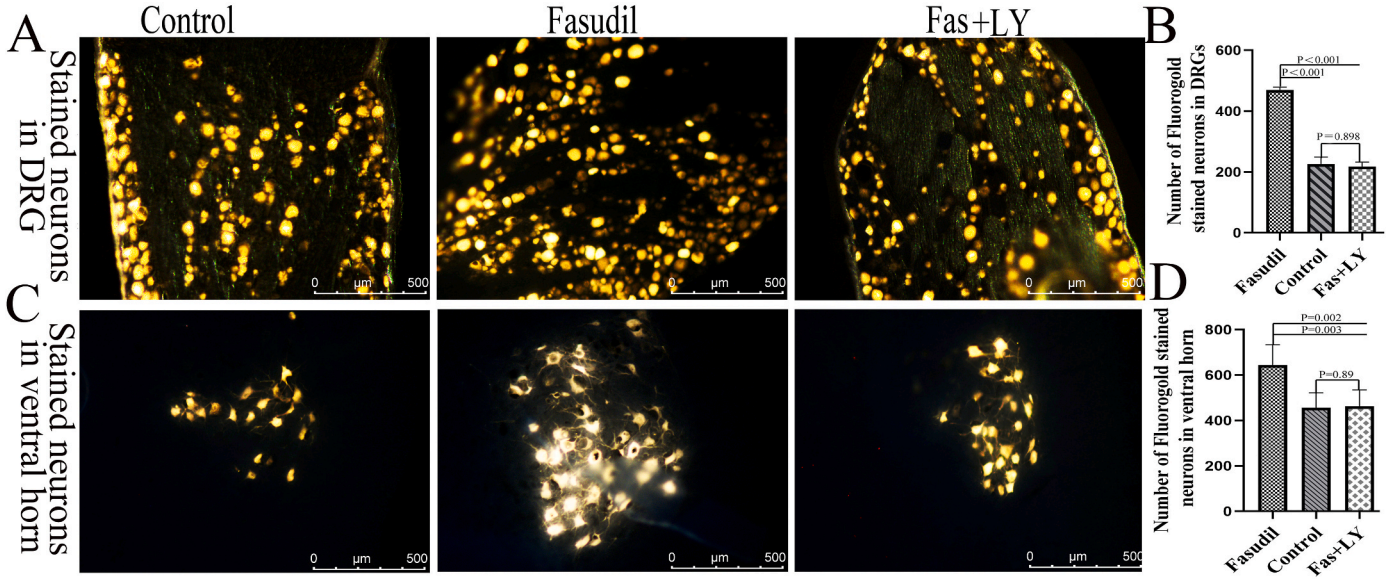

Fig. 5. Retrograde tracing of neurons with Fluoro-gold in the spinal cord and DRG. A and B showed that a significantly larger population of neurons marked by Fluoro-gold in $L_{4\text{-}6}$ DRG could be observed in the Fasudil group than that in the other two groups. C and D showed that a significantly larger population of neurons marked by Fluoro-gold in the lumbosacral enlargement could be observed in the Fasudil group than that in the other two groups. (For interpretation of the references to colour in this figure legend, the reader is referred to the Web version of this article.)

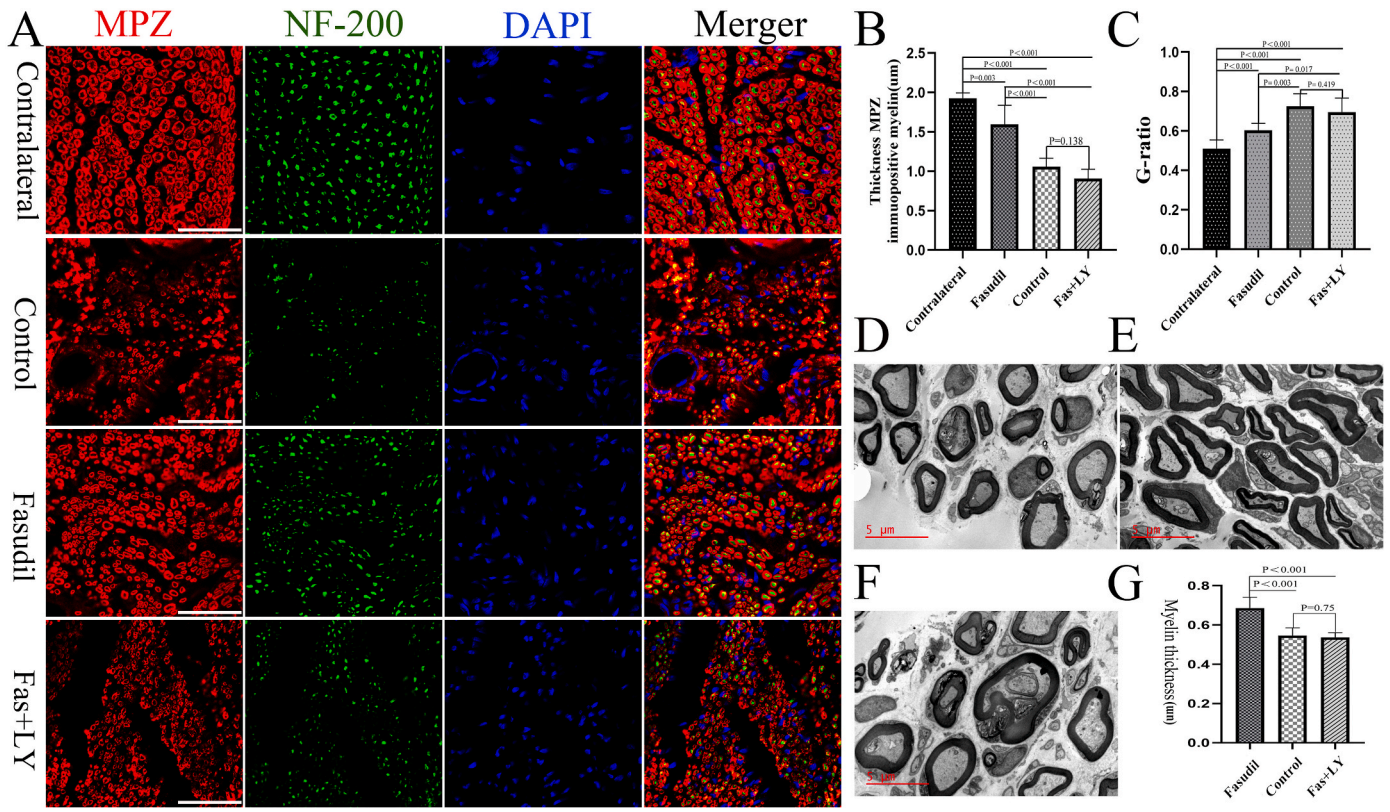

Fig. 6. Significant improvement of the thickness of remyelination by Fasudil three months after surgery. A was the co-immunostaining of myelin and axons. As could be observed, the myelin sheath in the Fasudil group had a more orderly configuration than that in the control and Fas + LY groups. Moreover, as showed by B and C, the myelin sheath in Fasudil group had a significantly larger thickness, and a significantly lower G-ratio as compared to that in the Control and Fas + LY groups, indicating a higher degree of maturity of regenerated axons in the Fasudil group. D, E, and F were the myelin sheath as observed by TEM in the control, Fasudil, and Fas + LY groups, respectively, which showed a more compacted arrangement of axons in the Fasudil group with a larger thickness of the myelin sheath as indicated by G. The bar denotes 50um.

was considered as statistically significant.

9. Results

9.1. Expression of ROCK2, P-PI3K and P-AKT after Fasudil application

At day 3 after model establishment, the expression of ROCK2 in the lumbosacral enlargement and $L_{4\text{-}6}$ DRG were significantly up-regulated ($P = 0.003$ and $P < 0.001$, Fig. 3A and B). Fasudil did not significantly repress the expression of the ROCK2 in the lumbosacral enlargement and the $L_{4\text{-}6}$ DRG ($P = 0.057$ and $P = 0.83$, Fig. 3C and D). Meanwhile, Fasudil did significantly raise the expression of p-PI3K and p-AKT in the lumbosacral enlargement and the $L_{4\text{-}6}$ DRG ($P < 0.05$, Fig. 3E–H).

9.2. Fasudil could significantly augment axon regeneration and LY294002 could abolish it

From both the longitudinal and cross sectioning of the sciatic nerve, it was distinct that there was more intensive NF-200 immunopositive staining in the Fasudil group. In the proximal sections, the density of axons in the Fasudil group was 77 ± 59 %, significantly larger than 62 ± 9 % and 55 ± 5 % in the control and Fas + LY groups ($P < 0.05$), respectively. In the middle sections, the density of axons was 72 ± 9 % in the Fasudil group, a slight decline from the proximal sections, still significantly larger than 41 ± 16 % and 39 ± 8 % in the control and Fas + LY groups($P < 0.01$), respectively, both witnessing a precipitous drop compared to that of their proximal sections. In the distal sections, the density became scarce, standing at 28 ± 10 % and 24 ± 7 %, respectively, in the control and Fas + LY groups, significantly lower than 45 ± 8 % in the Fasudil group($P < 0.01$) (Fig. 4).

In corroboration, the average number of neurons absorbing Fluoro-gold in the DRG of each rat in the Fasudil group was 470 ± 9, significantly larger than 225 ± 23 and 218 ± 15, respectively, in the control and Fas + LY groups ($P < 0.001$, Fig. 5A and B). In accordance, the average number of neurons absorbing Fluoro-gold in the ventral horn of the lumbosacral enlargement in the Fasudil group was 635 ± 10, significantly larger than 433 ± 44 and 436 ± 44, respectively, in the control and Fas + LY groups ($P < 0.001$, Fig. 5C and D)

9.3. Fasudil could significantly improve remyelination and LY294002 could abolish it

As shown by the co-immunostaining of MPZ and NF-200, the myelin sheath surrounding the axons in the contralateral uninjured side was orderly and evenly distributed, with a greater thickness than the regenerated myelin of the three groups ($P < 0.01$, Fig. 6A). In the Fasudil group, the myelin sheath was more compacted, greater in thickness, and more complete in its encirclement of axons when compared to that in the control and Fas + LY groups ($P < 0.05$, Fig. 6B). Moreover, the value of G-ratio was smaller in the Fasudil group in comparisons to that in the control and Fas + LY groups ($P < 0.05$, Fig. 6C), indicating a higher degree of maturity of axons. No significant difference in the thickness of myelin sheath and G-ratio could be detected between the control and Fas + LY groups ($P = 0.138$ and $P = 0.419$, Fig. 6B and C). In accordance, the myelin sheath in the Fasudil group as showed in TEM was thicker than in the other two groups ($P < 0.001$, Fig. 6D-G).

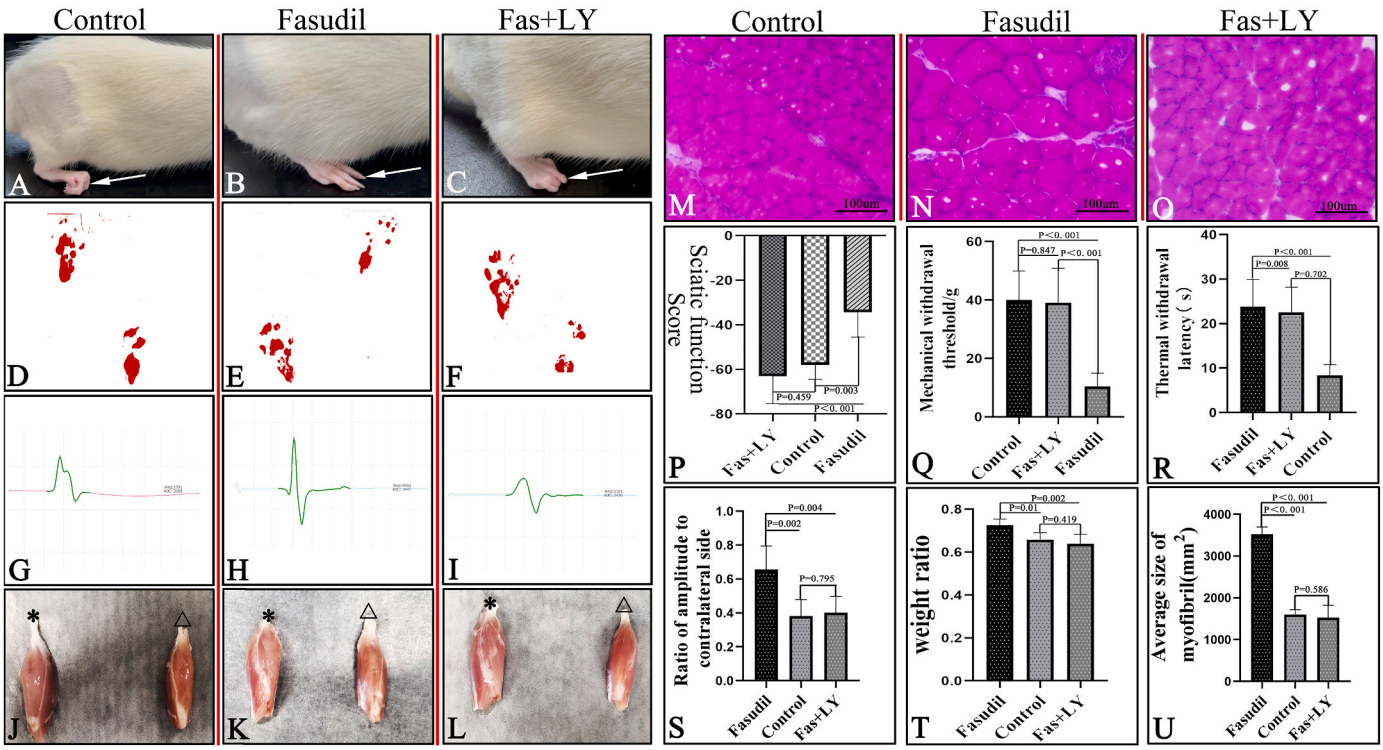

Fig. 7. Comparison of recovery of sensorimotor functions among the three groups. A, B, and C demonstrated the typical appearance of the right feet three months after surgery. The toes of the right feet in the control and Fas + LY groups often maintained a plantar flexion and could not have a full spread in contrast to those in the Fasudil group. D, E, and F showed the footprints of the right feet three months after surgery, and the SFI had a significantly higher value in the Fasudil group than that in the other two groups as indicated in P. Q and R showed that the right feet in the Fasudil group had a significant better recovery in sensing the mechanical and thermal stimuli than that in the other two groups. G, H, I and S demonstrated that Fasudil could significantly augment the amplitude of electrical impulse as could be observed in the other two groups. J, K and L demonstrated representative images of the Gastrocnemius from the right injured and left intact hind limbs, showing a significantly lower degree of atrophy in the Fasudil group (T), and M, N, an O demonstrated representative images of H&E staining of cross section of the Gastrocnemius, demonstrating a significantly larger cross-section area of individual myofibril in the Fasudil group (U). * and △ denote the muscle in the uninjured left limb, and the right injured limb of the same rat, respectively.

9.4. Fasudil could significantly improve the functional recovery and LY294002 could abolish it

At 12w after surgery, the toes of the right hind limb in the Fasudil group could have a full spread on the ground, whereas they often maintained a plantar flexion in the Control and Fas + LY groups (Fig. 7A–C). This could be corroborated by the result of footprints. In the Fasudil group, a greater length of the sole and clearly-demarcated digits and footpads could be observed, which was otherwise not discernible in the other two groups (Fig. 7D–F). The difference in footprints was quantitatively reflected as a much higher value of SFI in the Fasudil group, indicating a better recovery of motor function at 12w after model establishment ($P < 0.01$, Fig. 7P). In accordance, the tests using Von Frey filaments and Hot Plate both pointed to a lower threshold for sensing the mechanical and thermal stimuli in the Fasudil group ($P < 0.001$ and $P < 0.01$, Fig. 7Q and R). The better motor function was again supported by the motor-evoked potential, which revealed significantly higher amplitude in the Fasudil group ($P < 0.01$, Fig. 7G–I,S).

Compared to the control and Fas + LY groups, the atrophy of the Gastrocnemius in the Fasudil group was conspicuously attenuated, manifesting as a significantly larger wet weight ratio($P < 0.05$, Fig. 7J-L, T). For further confirmation of the extent of atrophy, the cross-section size of the individual myofibril was 1598 ± 117 um^2, 3524 ± 172 um^2, and 1524 ± 300 um^2, respectively, in the control, Fasudil, and Fas + LY groups (Fig. 7M–N). The average cross-section area of the myofibril in the Fasudil group was significantly greater than that in the control and Fas + LY groups ($P < 0.001$, Fig. 7U).

9.5. Fasudil could significantly preserve the morphology of the neuromuscular junction

The mammalian neuromuscular junction (NMJ) is a peripheral synapse that functionally couples lower motor neurons to the acetylcholine receptors in skeletal muscle fibers, and its degeneration is a hallmark after peripheral axotomy. In the contralateral side, an abundance of large-caliber nerve fibers could be observed, and in every section nearly all acetylcholine receptors were connected to the terminal ends of axons. Most of the acetylcholine receptors were round or oval in shape, with an average area of 4.7 ± 0.8 um^2. Due to the thickness of tissue section (100um), high-resolution pretzel-like configuration could only be observed in a few receptors. In comparison, the ratio of acetylcholine receptors connected with the terminal ends of axons was (68 ± 10) % in the Fasudil group, which, though lower than that in the contralateral side, was significantly higher than (48 ± 13) % and (42 ± 7) %, respectively, in the control and Fas + LY groups ($P < 0.01$). In accordance, due to poor regeneration of axons, the receptors underwent considerable shrinkage in the control group, with an average area of 2.1 ± 0.3um^2. However, significant shrinkage in the area of receptors could not be observed in the Fasudil and Fas + LY groups, strongly indicating that Fasudil could probably ameliorate the degeneration of acetylcholine receptors after peripheral nerve injury (Fig. 8).

9.6. Fasudil could significantly boost axon outgrowth of DRG by activating the PI3K/Akt pathway

Due to the aggregation of thousands of neurons within a DRG that sent out axons simultaneously, the configuration of a DRG in culture was

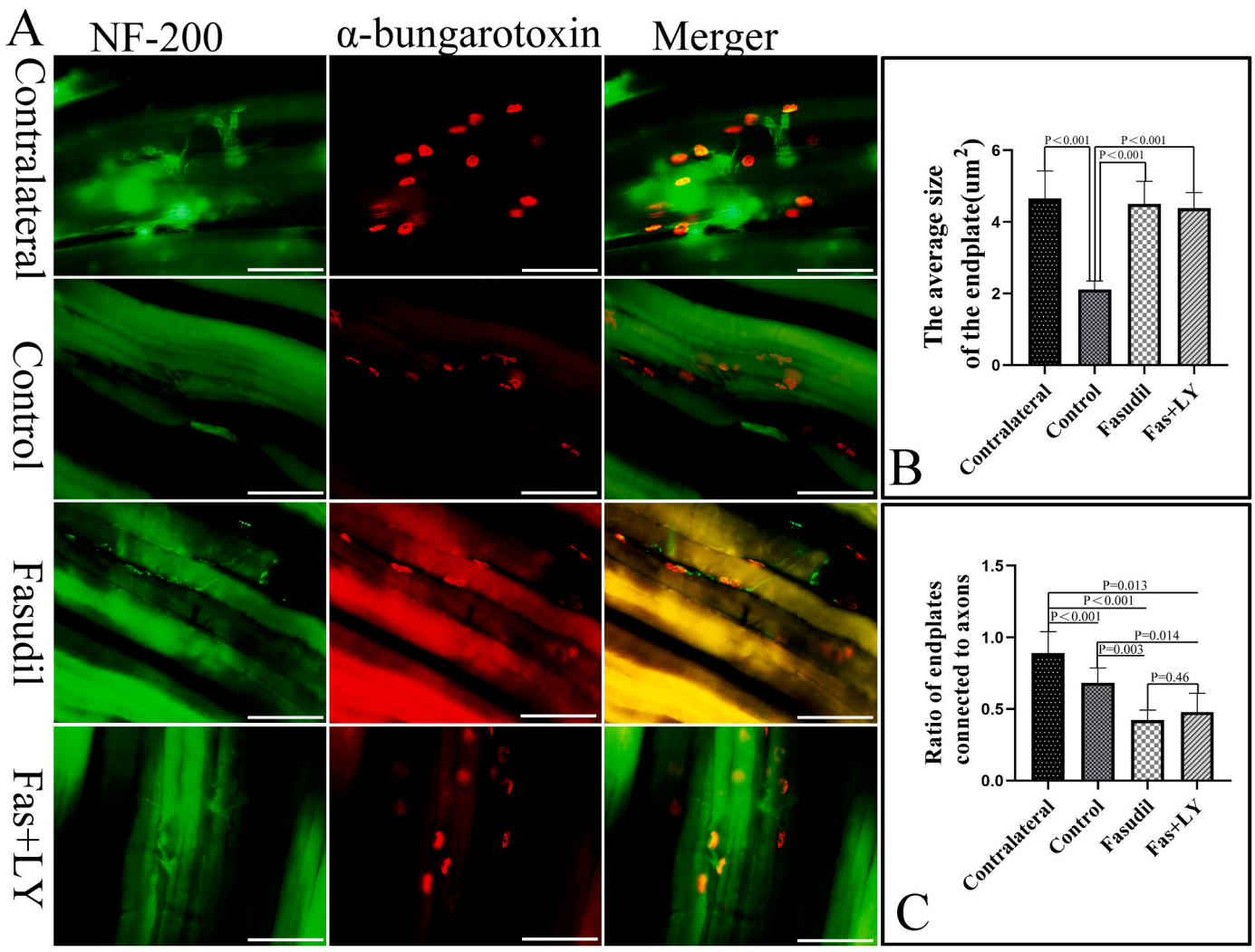

Fig. 8. Significantly better preservation of the morphology of the neuromuscular junction by Fasudil in the Gastrocnemius. As could be observed in A, The acetylcholine receptors as labeled by α-bungarotoxin had larger size and more connections to axons as compared to those in the control group. However, though application of LY294000 rendered axons scarcer in the muscle, the average size of acetylcholine receptors was not significantly reduced as compared to that in the Fasudil group as indicated in B and C. The bar denotes 250um.

round in appearance with the cell bodies located in the center.

After 5 days of culture, there were statistically significant differences in the average axon length of the DRG among the control, Fasudil, Fas + LY groups, and among the CSPG, CSPG + F, and CSPG + F + LY groups ($P < 0.05$). Compared to the control group, Fasudil could significantly promote axon growth (4.39 ± 0.34 mm vs. 3.56 ± 0.3 mm, $P = 0.011$) (Fig. 9A and B), and this efficacy could be significantly inhibited by LY294002 (4.39 ± 0.34 mm vs. 3.7 ± 0.32 mm, $P = 0.031$) (Fig. 9C and G). In contrast, CSPG could significantly retard the axon growth compared to the control group (2.48 ± 0.22 mm vs. 3.56 ± 0.3 mm, $P < 0.001$) (Fig. 9D). And Fasudil could still promote axon growth in this hostile environment (2.98 ± 0.11 mm vs. 2.48 ± 0.22 mm, $P = 0.012$) (Fig. 9E), and this efficacy was again significantly inhibited by LY294002 (2.98 ± 0.11 mm vs. 2.51 ± 0.24 mm, $P = 0.042$) (Fig. 9G).

After 3 days of culture, the expression of p-PI3K and p-AKT in the Fasudil group were significantly higher than that in the control and Fas + LY groups ($P < 0.05$, Fig. 9H and I). The expression of p-PI3K and p-AKT in the CSPG + F group were higher than that in the CSPG and CSPG + F + LY groups ($P < 0.05$, Fig. 9J and K).

9.7. Fasudil could significantly boost axon outgrowth of SMNs by activating the PI3K/Akt pathway

As demonstrated by the immunostaining of Tuj1, ChAT, and NeuN, the SMNs had a purity of 93 %, 90 %, and 93 %, respectively (Fig. 10). The average axon length of SMNs after 5 days of culture was significantly different among the control, Fasudil, Fas + LY, CSPG, CSPG + F, and CSPG + F + LY groups ($P < 0.001$). Compared to the control group, Fasudil could significantly promote axon growth (443 ± 71um vs. 278 ± 36um, $P < 0.001$), and this efficacy could be abolished by LY294002 (443 ± 71um vs. 262 ± 42um, $P < 0.001$) (Fig. 11A–C, G). Compared to the control group, CSPG could significantly retard axon growth (166 ± 36um vs. 278 ± 36um, $P < 0.001$), and Fasudil could augment axon growth in this hostile environment (264 ± 40um vs. 166 ± 36um, $P < 0.001$), and again this efficacy was abolished by LY294002 (264 ± 40um vs. 189 ± 37um, $P < 0.001$) (Fig. 11D–F, G).

After 3 days of culture, the expression of p-PI3K and p-AKT in the Fasudil group was higher than that in control group and Fas + LY group, and the difference was statistically significant ($P < 0.05$, Fig. 11H and I). The expression of p-PI3K and p-AKT in the CSPG + F group was significantly higher than that in the CSPG and CSPG + F + LY groups ($P < 0.05$, Fig. 11J and K).

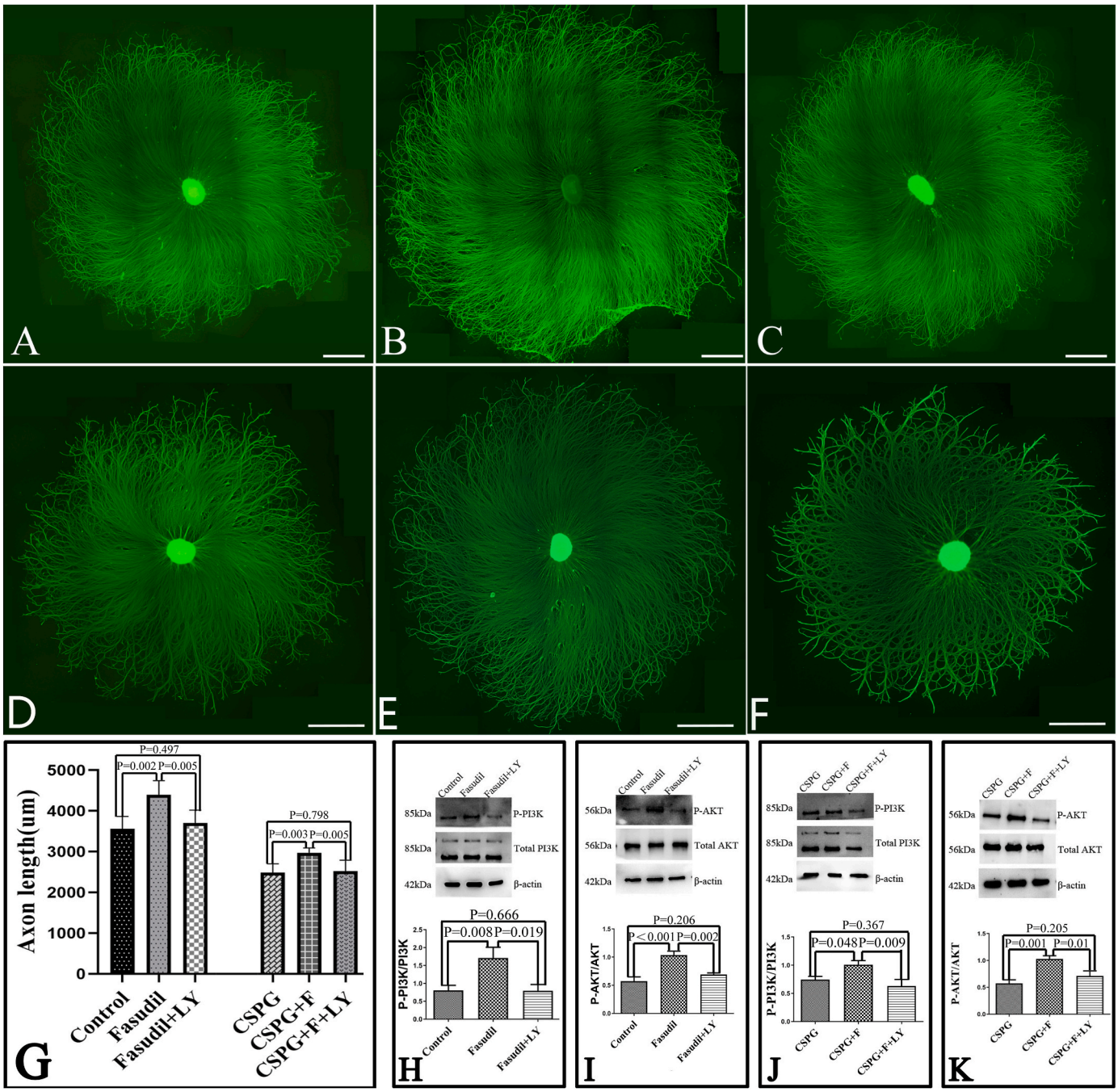

Fig. 9. Fasudil could significantly improve axon outgrowth of DRG in both permissive and non-permissive substrates. A, B, and C were the representative images of the DRG from the control, Fasudil, and Fas + LY groups at day 5 after culturing in permissive PDL substrate, respectively. D, E, and F were the representative images of the DRG from CSPG, CSPG + F, and CSPG + F + LY groups at day 5 after culturing in non-permissive PDL + CSPG substrate, respectively. The bar denotes 500um. G, significantly longer axons could be observed in the Fasudil group and in the GSPG + Fasudil group compared to those in the other two groups, respectively. H indicated usage of Fasudil could up-regulate the phosphorylation level of PI3K and AKT in the permissive substrate; J and K indicated usage of Fasudil could up-regulate the phosphorylation level of PI3K and AKT in the non-permissive substrate.

10. Discussion

Peripheral nerve injury have been classified by scientists into different grades depending upon the severity. Seddon classified the PNIs into 3 grades on the basis of the presence of demyelination and the extent of damage to the axons and the connective tissue of the nerve. Sunderland then gave further subdivision on the basis of discontinuity of several layers of connective tissues in the peripheral nerve [24]. By any classification, complete severance is the most severe form of injury to a nerve that will result in a total loss of the function of target organs and has the poorest recovery after coaptation due to the discontinuity of endoneurial channels. Therefore, we choose to examine the pro-regeneration efficacy of Fasudil on a PNI model with complete transection of the sciatic nerve in rats, unlike a previous report examining the efficacy of Fasudil on a crush injury model in mice [25].

Fasudil is an inhibitor of ROCK, a substrate of Rho A, which is a member of Rho guanosine triphosphatases (GTPases) that are a family of highly related proteins best characterized by their effects on the actin cytoskeletons [11,12]. Several Rho isoforms have been reported, and RhoA is expressed at higher levels than RhoB and RhoC in neurons. Rho

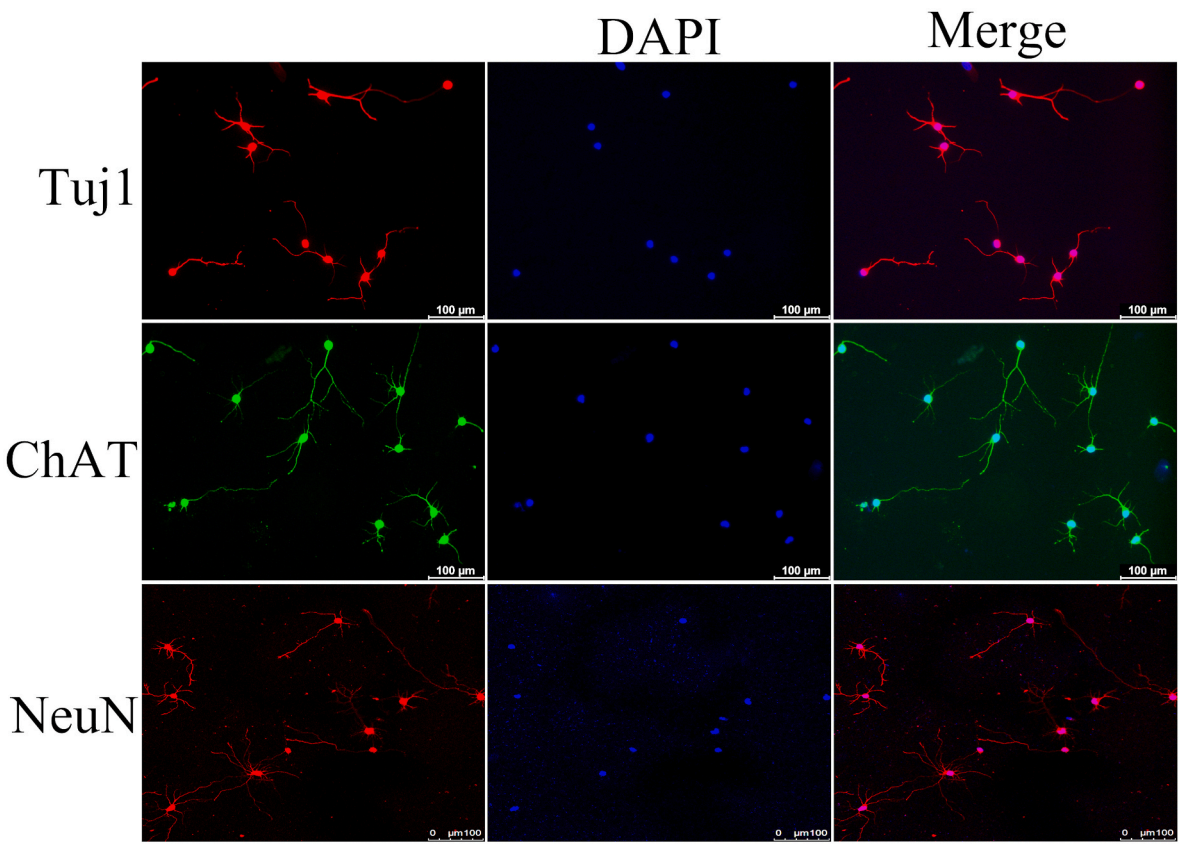

Figure 10. Identification of the purity of SMNs. Three markers, Tuj 1, ChaT and NeuN, all pointed to the higher purity of SMNs extracted using the immunopanning approach.

family members signal to the actin cytoskeleton through the main effector ROCK [26]. In the central regenerative microenvironment, numerous studies have demonstrated that the myelin-associated molecules Nogo-66, myelin-associated glycoprotein, and oligodendrocyte myelin glycoprotein or CSGP can trigger RhoA GTPase activation, and induce growth cone collapse [27,28]. Comparatively, there are far fewer exploration at the impact of the RhoA/ROCK signaling in the peripheral nervous system.

As demonstrated in this study, the expression of ROCK2, the main isoform in the nervous system, was significantly up-regulated at day 3 after surgery in both the $L_{4\text{-}6}$ DRG and the lumbosacral enlargement that send axons into the sciatic nerve. This up-regulation of ROCK2 could be triggered by an increased production of CSPG and the myelin-associated glycoproteins by Schwann cells [29], justifying our application of Fasudil as an attempt to promote axon outgrowth. However, Fasudil did not directly reduce the expression of ROCK2, as a reduced expression of ROCK2 after application of Fasudil could not be observed, indicating that Fasudil might just binds to the active domain of ROCK and interfere with its activity.

Past researches regarding the efficacy of ROCK inhibitors on the peripheral nerve regeneration have never attempted to delineate the potential downstream pathways. Here we demonstrated in vivo that the phosphorylation of PI3K and AKT was significantly increased after usage of Fasudil at day 3 after surgery. Meanwhile, after application of Fasudil into the culture medium of DRG explants and SMNs in both the permissive substrate and the non-permissive substrate, the same phenomenon of increased phosphorylation of PI3K and AKT could be observed. The in vivo and in vitro results both indicate that inhibition of ROCK using Fasudil can result in activation of the PI3K/AKT pathway that is involved in the augmentation of axon outgrowth after injury. The results are in accordance with our previous study investigating efficacy of Fasudil on flap survival and reinnervation [30].

In the sciatic nerve transection model, it was showed that Fasudil demonstrated a remarkable efficacy at enhancing the density of axons at longitudinal and cross sections of the sciatic nerve. The retrograde tracing revealed that a significantly larger number of the motor neurons in the ventral horn of the lumbosacral enlargement and of the sensory neurons in the $L_{4\text{-}6}$ DRG absorbed Fluoro-gold in the Fasudil group, implying that the greater density of axons are attributed to a larger number of neurons sending their axons across the transection site instead of increased collateral sprouting. Therefore, it can be concluded that Fasudil could simultaneously promote the regeneration of motor and sensory axons. In corroboration, Fasudil added to the culture medium could not only augment the axon outgrowth of DRG explants and SMNs in permissive substrate, but also in non-permissive substrate where the axons were severely retarded by CSPG. Our results differ a little bit from the findings of Joshi et al. [29], who concluded that Y27632, another ROCK inhibitor, could only augment axon outgrowth of motor neurons but had no efficacy on DRG neurons. The difference might be caused by (1) different culture methods of DRG neurons used, i.e., pure dissociated DRG neurons were used in their research, whereas DRG explants were adopted in this study, and (2) the different degrees of specificity of the two Rho kinase inhibitors that might target other kinases, such as PKA, PKG, PKC and MLCK [31,32].

In sync with the protein expression assays showing the activation of the PI3K/AKT pathway, inhibition of the pathway using LY294002 completely abolished the efficacy of Fasudil, thus providing a direct evidence to the involvement of the PI3K/AKT pathway in mediating the axon-promoting function of Fasudil. Several studies have demonstrated that the PI3K/AKT pathway plays a crucial role in influencing axon ougrowth by modulating the microtubule dynamics in the growth cone through GSK3. GSK-3 is a glycogen synthase kinase, a multifunctional serine/threonine kinase initially recognized as a negative regulator of glucose metabolism. It has two isoforms, GSK-3α and GSK-3β. With

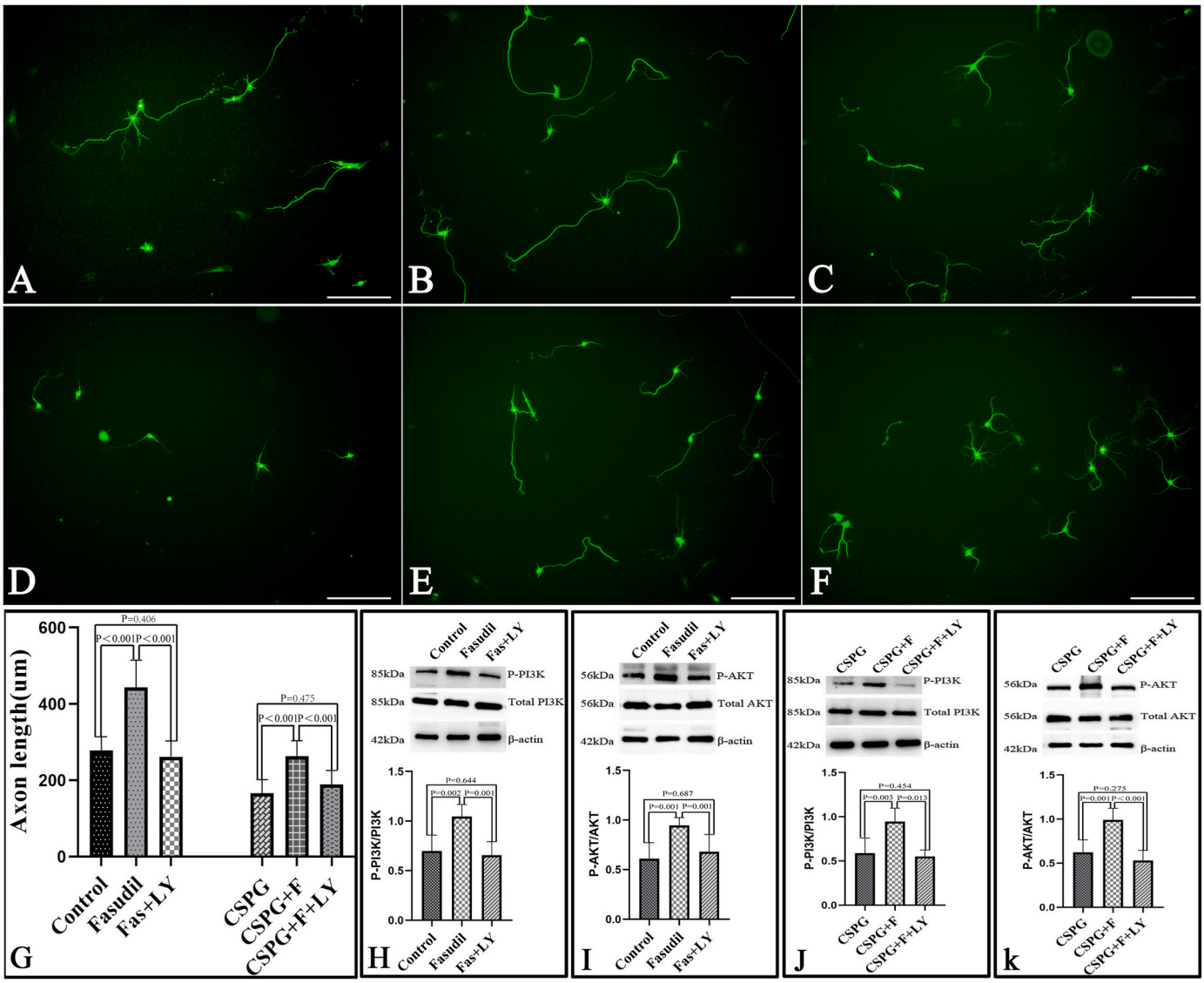

Figure 11. Fasudil could significantly improve axon outgrowth of SMNs in both permissive and non-permissive substrates. A, B, and C were the representative images of SMNs from the control, Fasudil, and Fas + LY groups at day 5 after culturing in permissive PDL + laminin substrate, respectively. D, E, and F were the representative images of SMNs from CSPG, CSPG + F, and CSPG + F + LY groups at day 5 after culturing in non-permissive PDL + laminin + CSPG substrate, respectively. The bar denotes 500um. G, significantly longer axons could be observed in the Fasudil group and in the GSPG + F group compared to those in the other two groups, respectively. H indicated usage of Fasudil could up-regulate the phosphorylation level of PI3K and AKT in the permissive substrate; J and K indicated usage of Fasudil could up-regulate the phosphorylation level of PI3K and AKT in the non-permissive substrate.

deeper understanding, GSK-3β is now considered to play an extreme important role in neurogenesis, neurite growth and plasticity [33,34]. Activation of AKT can result in inhibition of GSK-3β by phosphorylation at serine 9 or 21 [35], which can lead to dephosphorylation of microtubule-associated proteins, such as CRMP-2, MAP1B and APC, increasing their affinity to the microtubules to promote axon outgrowth [36–38]. Another optional way for the activated PI3K/AKT to promote axon outgrowth is to activate the transcription factor Smad-1, which then up-regulates the expression of SPRR1, ATF3, c-Jun and GAP43, all axon regeneration-associated factors that can promote axon regeneration [39]. Therefore, the future focus is to identify the exact downstream of PI3K/AKT that mediates the efficacy of Fasudil.

As showed by the staining of the neuromuscular junction, the overall greater density of axons in the nerve trunk has translated to a greater ratio of acetylcholine receptors with axon connection in the Fasudil group, which further resulted in a better preservation of the morphology of the acetylcholine receptors, preventing it from degradation. However, compared to the axons within the contralateral uninjured limb, axons within the Gastrocnemius were still less abundant and smaller in diameter in the Fasudil group, leaving room for future exploration of combination therapy to achieve better results. A better innervation of the muscle in the Fasudil group was also reflected in a much better results of foot stepping on the ground and a lesser degree of muscle atrophy compared to the other two groups. The other interesting observation is that though LY294002 inhibited the axon-promoting efficacy of Fasudil manifested as a lower ratio of axon-acetylcholine receptor junction, there was no difference between the average size of the receptors in the Fasudil and Fas + LY groups, implying that Fasudil can attenuate the degradation of the receptors even without augmenting the axon-acetylcholine receptor junction. This observation need to be further corroborated, and the underlying mechanism need to be investigated.

As one of the most important proteins that regulate the cytoskeletons, RhoA has been widely studied in the regulation of Schwann cell biology. Melendez-Vasquez pointed out that inhibition of RhoA/ROCK in a coculture system using DRG neurons and Schwann cells would result

in abnormal short and independent myelin segments along the length of axons, each with associated nodes and paranodes, resembling myelin formed by oligodendrocytes [40]. Wen showed that Rho A activity was increased during the in vitro differentiation of Schwann cells induced by db-cAMP. Inhibiting of RhoA could inhibit the differentiation of Schwann cells, reducing the expression of genes associated with differentiated and mature Schwann cells such as Krox20, MAG, and PMP22, and increasing the expression of markers of dedifferentiated and immature Schwann cells such as c-JUN, Sox2, and P75 [41]. Dan showed in vitro that inhibition of Rho A with C3 transferase in Schwann cells inhibited their proliferation through inactivation of PTEN/PI3K/AKT instead of activation of ROCK, because adding Y27632 to inhibit ROCK activity did not significantly affect Schwann cell proliferation [42]. The above-mentioned studies were all conducted in vivo, therefore do not necessarily reflect the effects of ROCK inhibitor, especially Fasudil, on myelination in vivo. Our studies shows that Fasudil application can increase the thickness of myelination around the axons, though this may be a "side effect" of better axon outgrowth in the Fasudil group. In order to have a clear picture of the effect of ROCK inhibitor on remyelination, PNI model should be established on mice with conditional knockout of ROCK in schwann cells so that the axon regeneration-promoting effects on remyelination can be ruled out.

An obvious shortcomings of this study is that we are unable to delineate the exact way in which inhibition of ROCK with Fasudil can increase the phosphorylation of PI3K/AKT. A lot of work remains to be done to investigate whether there is a direction interaction between ROCK and PI3K or there is an intermediator.

In conclusions, our study has a first comprehensive demonstration of the remarkable efficacy of Fasudil at augmenting axon regeneration, remyelination, and improving sensory and motor function in a rat sciatic nerve-transection injury model. The other noteworthy point is that the PI3K/AKT pathway serves as a downstream node for Fasudil to achieve its efficacy. **Taking into consideration that Fasudil has been successfully implemented into clinical practice for the treatment of subarachnoid hemorrhage in Japan and China, guaranteeing its safety, we opine that our study has a great translational potential to be used clinically to treat peripheral nerve injury.**

Funding

The study was funded by Natural Science Fundation of Fujian Province (No.2021J01241, 2021J01666) and Joint Funds for the Innovation of Science and Technology, Fujian Province (No.2021Y9091).

Disclosure

This paper has not been published in any other journal, neither is it presented in any meeting. All authors have approved the manuscript and agree with submission to ***Journal of orthopaedic translation***. The authors have no conflicts of interest to declare.

Acknowledgements

Thanks to the support from Natural Science Fundation of Fujian Province and Joint Funds for the Innovation of Science and Technology, Fujian Province.

References

[1] Benga A, Zor F, Korkmaz A, Marinescu B, Gorantla V. The neurochemistry of peripheral nerve regeneration. Indian J Plast Surg official publication of the Association of Plastic Surgeons of India 2017;50(1):5–15.
[2] Lavorato A, Aruta G, De Marco R, Zeppa P, Titolo P, Colonna MR, et al. Traumatic peripheral nerve injuries: a classification proposal. J Orthop Traumatol : official journal of the Italian Society of Orthopaedics and Traumatology 2023;24(1):20.
[3] Lin J, Shi J, Min X, Chen S, Zhao Y, Zhang Y, et al. The GDF11 promotes nerve regeneration after sciatic nerve injury in adult rats by promoting axon growth and inhibiting neuronal apoptosis. Front Bioeng Biotechnol 2021;9:803052.
[4] Sulaiman W, Gordon T. Neurobiology of peripheral nerve injury, regeneration, and functional recovery: from bench top research to bedside application. Ochsner J 2013;13(1):100–8.
[5] Paramel Mohan S, Ramalingam M. Neuroscience of peripheral nerve regeneration. J Pharm BioAllied Sci 2021;13(Suppl 2):S913–6.
[6] Wariyar SS, Ward PJ. Application of electrical stimulation to enhance axon regeneration following peripheral nerve injury. Bio-protocol 2023;13(19):e4833.
[7] Guo S, Moore RM, Charlesworth MC, Johnson KL, Spinner RJ, Windebank AJ, et al. The proteome of distal nerves: implication in delayed repair and poor functional recovery. Neural regeneration research 2022;17(9):1998–2006.
[8] Wagstaff LJ, Gomez-Sanchez JA, Fazal SV, Otto GW, Kilpatrick AM, Michael K, et al. Failures of nerve regeneration caused by aging or chronic denervation are rescued by restoring Schwann cell c-Jun. Elife 2021;10.
[9] Benito C, Davis CM, Gomez-Sanchez JA, Turmaine M, Meijer D, Poli V, et al. STAT3 controls the long-term survival and phenotype of repair schwann cells during nerve regeneration. J Neurosci : the official journal of the Society for Neuroscience 2017;37(16):4255–69.
[10] Gordon T. Peripheral nerve regeneration and muscle reinnervation. Int J Mol Sci 2020;21(22).
[11] Choi EK, Kim JG, Kim HJ, Cho JY, Jeong H, Park Y, et al. Regulation of RhoA GTPase and novel target proteins for ROCK. Small GTPases 2020;11(2):95–102.
[12] Hall A, Lalli G. Rho and Ras GTPases in axon growth, guidance, and branching. Cold Spring Harbor Perspect Biol 2010;2(2):a001818.
[13] Mulherkar S, Tolias KF. RhoA-ROCK signaling as a therapeutic target in traumatic brain injury. Cells 2020;9(1).
[14] Lu XC, Zheng JY, Tang LJ, Huang BS, Li K, Tao Y, et al. MiR-133b promotes neurite outgrowth by targeting RhoA expression. Cellular Physiology & Biochemistry International Journal of Experimental Cellular Physiology Biochemistry & Pharmacology 2015;35(1):246–58.
[15] Gu X, Meng S, Liu S, Jia C, Fang Y, Li S, et al. miR-124 represses ROCK1 expression to promote neurite elongation through activation of the PI3K/akt signal pathway. Springer US; 2014. 1.
[16] Maruhashi T, Higashi Y. An overview of pharmacotherapy for cerebral vasospasm and delayed cerebral ischemia after subarachnoid hemorrhage. Expet Opin Pharmacother 2021;22(12):1–14.
[17] Wang Q, Song LJ, Ding ZB, Chai Z, Yu JZ, Xiao BG, et al. Advantages of Rho-associated kinases and their inhibitor fasudil for the treatment of neurodegenerative diseases. neural regeneration research 2022;17(12).
[18] Sato K, Nakagawa S, Morofuji Y, Matsunaga Y, Fujimoto T, Watanabe D, et al. Effects of fasudil on blood-brain barrier integrity. Fluids Barriers CNS 2022;19(1):43.
[19] Impellizzeri D, Mazzon E, Paterniti I, Esposito E, Cuzzocrea S. Effect of fasudil, a selective inhibitor of Rho kinase activity, in the secondary injury associated with the experimental model of spinal cord trauma. J Pharmacol Exp Therapeut 2016;343(1):21–33.
[20] Fukuta T, Asai T, Sato A, Namba M, Yanagida Y, Kikuchi T, et al. Neuroprotection against cerebral ischemia/reperfusion injury by intravenous administration of liposomal fasudil. Int J Pharm 2016;506(1–2):129–37.
[21] Huang L., Li Q., Wen R., Yu Z., Li N., Ma L., et al. Rho-kinase inhibitor prevents acute injury against transient focal cerebral ischemia by enhancing the expression and function of GABA receptors in rats. Eur J Pharmacol 2017 Feb 15;797:134-142.
[22] Shekarabi M, Robinson JA, Burdo TH. Isolation and culture of dorsal root ganglia (DRG) from rodents. Methods Mol Biol 2021;2311:177–84.
[23] Graber DJ, Harris BT. Purification and culture of spinal motor neurons from rat embryos. Cold Spring Harbor protocols 2013;2013(4):319–26.
[24] Hussain G, Wang J, Rasul A, Anwar H, Sun T. Current status of therapeutic approaches against peripheral nerve injuries: a detailed story from injury to recovery. Int J Biol Sci 2020;16(1):116–34.
[25] Rho-kinase inhibition enhances axonal regeneration after peripheral nerve injury. J Peripher Nerv Syst 2006;11(3).
[26] Stankiewicz TR, Linseman DA. Rho family GTPases: key players in neuronal development, neuronal survival, and neurodegeneration. Front Cell Neurosci 2014;8:314.
[27] Niederoest B, Oertle T, Fritsche J, Bandtlow C. Nogo-A and myelin-associated glycoprotein mediate neurite growth inhibition by antagonistic regulation of RhoA and Rac1. 2003.
[28] Tan HB, Zhong YS, Cheng Y, Shen X. Rho/ROCK pathway and neural regeneration: a potential therapeutic target for central nervous system and optic nerve damage. International Eye Science 2011;(6):6.
[29] Joshi AR, Bobylev I, Zhang G, Sheikh KA, Lehmann HC. Inhibition of Rho-kinase differentially affects axon regeneration of peripheral motor and sensory nerves. Exp Neurol 2015;263:28–38.
[30] Wang H, Fang F, Chen S, Jing X, Zhuang Y, Xie Y. Dual efficacy of Fasudil at improvement of survival and reinnervation of flap through RhoA/ROCK/PI3K/Akt pathway. Int Wound J 2022;19(8):2000–11.
[31] Chen M, Liu A, Ouyang Y, Huang Y, Chao X, Pi R. Fasudil and its analogs: a new powerful weapon in the long war against central nervous system disorders? Expert Opin Investig Drugs 2013;22(4):537–50.
[32] Koch J.C., Kuttler J., Maass F., Lengenfeld T., Zielke E., Bhr M., et al. Compassionate use of the ROCK inhibitor fasudil in three patients with amyotrophic lateral sclerosis. Front Neurol 2020 Mar 13;11:173.
[33] Jung EM, Ka M, Kim WY. Loss of GSK-3 causes abnormal astrogenesis and behavior in mice. Mol Neurobiol 2016;53(6):3954–66.
[34] Li J, Ma S, Chen J, Hu K, Li Y, Zhang Z, et al. GSK-3beta contributes to parkinsonian dopaminergic neuron death: evidence from conditional knockout mice and tideglusib. Front Mol Neurosci 2020;13:81.

[35] Tan M, Ma S, Huang Q, Hu K, Song B, Li M. GSK-3alpha/beta-mediated phosphorylation of CRMP-2 regulates activity-dependent dendritic growth. J Neurochem 2013;125(5):685–97.
[36] Leibinger M, Hilla AM, Andreadaki A, Fischer D. GSK3-CRMP2 signaling mediates axonal regeneration induced by Pten knockout. Commun Biol 2019;2:318.
[37] Hajka D, Budziak B, Pietras L, Duda P, McCubrey JA, Gizak A. GSK3 as a regulator of cytoskeleton architecture: consequences for Health and disease. Cells 2021;10 (8).
[38] Valvezan AJ, Zhang F, Diehl JA, Klein PS. Adenomatous polyposis coli (APC) regulates multiple signaling pathways by enhancing glycogen synthase kinase-3 (GSK-3) activity. J Biol Chem 2012;287(6):3823–32.
[39] Saijilafu Hur EM, Liu CM, Jiao Z, Xu WL, Zhou FQ. PI3K-GSK3 signalling regulates mammalian axon regeneration by inducing the expression of Smad1. Nat Commun 2013;4:2690.
[40] Melendez-Vasquez CV. Rho kinase regulates schwann cell myelination and formation of associated axonal domains. Journal of Neuroscience the Official Journal of the Society for Neuroscience 2004;24(16):3953.
[41] Jinkun W, Dandan T, Lixia L, Xianghai W, Mengjie P, Jiasong G. RhoA regulates Schwann cell differentiation through JNK pathway. Exp Neurol 2018;308:26–34.
[42] Tan D, Wen J, Li L, Wang X, Qian C, Pan M, et al. Inhibition of RhoA-subfamily GTPases suppresses schwann cell proliferation through regulating AKT pathway rather than ROCK pathway. Front Cell Neurosci 2018;12:437.